

Original Research Article**Natural Products Screening for the Identification of Selective Monoamine Oxidase-B Inhibitors****ABSTRACT**

Aims: Monoamine oxidase-B inhibitors(MAO-BI) are used for the initial therapy of Parkinson disease. Also, MAO-BI showed effective neuroprotective abilities in several neurodegenerative diseases. However, some concerns existed about their long-term use. Nevertheless, natural compounds showed potential MAO-B selective inhibitions. To date, few selective and natural MAO-B inhibitors have been identified. Therefore, the current study is designed to identify plants with potent and specific MOA-B inhibition.

Study Design: In this work, we utilized high throughput screening to evaluate the different plants ethanolic extract for their effectiveness to inhibit *recombinant human (h)MAO-A* and *hMAO-B* and to determine the relative selectivity of the top MAO-BI.

Methodology: Recombinant human isozymes were verified by Western blotting, and the 155 plants were screened. A continuous fluorometric screening assay was performed followed by two separate *hMAO-A* and *hMAO-B* microtiter screenings and IC_{50} determinations for the top extracts.

Results: From the screened plants, 9% of the extracts showed > 1.5-fold relative inhibition of *hMAO-B* (RI_B) and another 9% with > 1.5-fold relative inhibition of *hMAO-A*. The top extracts with the most potent RI_B s were *Psoralea corylifolia* seeds, *Phellodendron amurense* bark, *Glycyrrhiza uralensis* roots, and *Ferula assafoetida* roots, with the highest RI_B of 5.9-fold. Furthermore, extensive maceration of the promising extracts led to an increased potency with a preserved RI_B as confirmed with luminescence assay. The four extracts *hMAO-B* inhibitions were equally potent (IC_{50} = 1.3 to 3.8 μ g/ml) with highly significant relative selectivities to inhibit *hMAO-B* (4.1- to 13.4-fold).

Conclusion: The obtained results indicate that *Psoralea corylifolia* seeds, *Ferula assafoetida*, and *Phellodendron amurense* ethanolic extracts have potent and selective inhibition for MAO-BIs. Highlighting these extracts as natural sources for novel MAO-BIs to be investigated for their therapeutic use in neurodegenerative diseases including Parkinson's disease.

Keywords: Parkinson disease, selective monoamine oxidase-B inhibitors, *Psoralea corylifolia* seeds, *Phellodendron amurense*, *Glycyrrhiza uralensis*, *Ferula assafoetida*.

36 **ABBREVIATIONS**

37	EEs	ethanolic extracts
38	RS _B	relative selectivity for <i>h</i> MAO-B inhibition
39	tyr. HCl	p-tyramine HCl
40	benz. HCl	benzylamine HCl
41	SNpc	substantia nigra pars compacta
42	SN	substantia nigra
43	RI	relative inhibition
44	RI _B	relative <i>h</i> MAO-B inhibitor
45	AD	Alzheimer's disease
46	DEP	selegiline (Deprenyl [®])
47	H ₂ O ₂	hydrogen peroxide
48	EOH	ethanol
49	PCS	<i>Psoralea corylifolia</i> seeds
50	PAB	<i>Phellodendron amurense</i> barks
51	FAR	<i>Ferula assafoetida</i> resins
52	GUR	<i>Glycyrrhiza uralensis</i> roots
53	PCSEE	<i>Psoralea corylifolia</i> seeds ethanolic extract
54	PABEE	<i>Phellodendron amurense</i> barks ethanolic extract
55	FAREE	<i>Ferula assafoetida</i> resins ethanolic extract
56	GUREE	<i>Glycyrrhiza uralensis</i> roots ethanolic extract
57	MAO	monoamine oxidase
58	<i>h</i> MAO-A	recombinant human monoamine oxidase-A
59	<i>h</i> MAO-B	recombinant human monoamine oxidase-B
60	HTS	high throughput screening
61	NE	norepinephrine

62 **1. INTRODUCTION**

63 In Parkinson's disease (PD) and depression, monoamine oxidase-A and B inhibitors (MAO-AIs and
64 MAO-BIs) are currently used as effective drugs. MAO-A and MAO-B are two isozymes belong to the
65 Flavin-containing amine oxidases that can be found in astrocytes and the substantia nigra pars
66 compacta (SNpc) neurons to metabolize monoamine neurotransmitters. In PD, MAO-BIs are used to
67 increase neurotransmitter dopamine (DA), reduce oxidative stress level and relieve the psychomotor

68 disease symptoms [1]. Even though DA is well metabolized by both isozymes [2], MAO-B is more
69 specific in metabolizing the already depleted DA in the SNpc of the PD patients [3]. Additionally, the
70 activity of MAO-B is elevated up to three-fold in PD and Alzheimer's disease (AD) as compared to
71 normal levels [4]. That MAO-B elevation [1, 5] with the co-localized of active MAO-A isozyme can
72 potentially aggravate oxidative stress in aging patients. Both MAOs activities produce abnormally high
73 amounts of hydrogen peroxide (H_2O_2) and aldehydes that are neurotoxic. Those byproducts
74 potentially damage proteins, nucleic acids, lipids and activate apoptotic pathways [6]. Unfortunately,
75 the aldehyde dehydrogenase enzyme that metabolizes the neurotoxic aldehydes produced by the
76 active MAOs was found to be genetically deficient in PD patients' SNpc [7, 8]. Other oxidative stress
77 defense enzymes may also become limited with the overwhelming reactive species produced.
78 Consequently, these toxic byproducts, particularly of active MAO-B, can potentially accumulate in
79 neurons and astrocytes leading to cell death and aggravating neurodegeneration.

80 While MAO-AIs are usually associated with concerns about food and drug interactions that lead to
81 rare but serious side effects (the cheese effect and serotonin syndrome) [9, 10], MAO-BIs were found
82 ideal for the management of PD as in the case of selegiline (Deprenyl[®]) (DEP). These inhibitors were
83 proven to be clinically efficient for decades as they delayed the need for L-dopa in PD management.
84 Selective MAO-BIs may also inhibit the conversion of nontoxic xenobiotic substrates to neurotoxins in
85 the brain, such as the MPTP conversion to its neurotoxic product MPP+. MAO-BI also exerted anti-
86 apoptotic and other multifunctional neuroprotective activities [11] which led to extended PD patients'
87 life expectancy [8]. Moreover, MAO-BIs such as DEP were reported beneficial in other neurological
88 disorders such as cerebrovascular ischemia, Tourette syndrome, narcolepsy, and AD [12].

89 Although this may sound ideal for MAO-BI DEP in neurological diseases, some concerns exist with
90 their long-term use. Recent evidence of neurotoxic metabolite of DEP, L-methamphetamine, showed
91 contradictions in their antiparkinsonian action *in vitro* [13], and some attributed rare cases of tolerance
92 or dependence development on some MAOIs to their amphetamine-like metabolites structures [14].
93 Meanwhile, the currently available MAO-BIs are synthetic compounds that share common structures
94 such as DEP and rasagiline, clorgyline that contains N-propargyl, the responsible group for MAO
95 inhibition and neuroprotection [2]. On the other hand, it was reported that potent and selective MAO-
96 BIs in nature are commonly found to include flavonoids, β -carbolines, xanthenes, and alkaloids [15].

97 Therefore, new natural structures may promote the discovery of new lead compounds with unique
98 properties as in the classical MAO-BIs. To recognize if the total phytochemical constituents of plant
99 extracts also have the ability to selectively inhibit human MAO-B, high-throughput screening (HTS)
100 was conducted on both isozymes. Pointing out the plants with the most selective MAO-B inhibitory
101 properties may further reveal unique phytochemical structure properties with multifunctional
102 neuroprotective and neurorescue properties beneficial to neurodegenerative such as PD.

103 **2. METHODOLOGY**

104 **2.1. Materials**

105 The *h*MAO-A and *h*MAO-B isozymes, produced in BTI-TN-5B1-4 insect cells containing human cDNA,
106 and their analyzed active units (U), were purchased and identified by Sigma-Aldrich (St. Louis, MO,
107 USA). Isozymes stocks were diluted with 1% of 1 M HEPES in Hank's Balanced Salt Solution (HBSS)
108 (pH 7.4) and aliquots stored at -80°C for single use. Standards of pirlindole, a reversible inhibitor for
109 MAO-A (RIMA), deprenyl (DEP), an irreversible MAO-BI, and cell culture media and supplements
110 were also purchased from Sigma-Aldrich. Different plant parts were purchased from and identified by
111 their trades companies including, East Earth Trade Winds (Redding, CA, USA), Mountain Rose,
112 Herbs (Eugene, OR, USA), Mayway Corp. (Oakland, CA, USA), Monterey Bay Spice Comp.
113 (Watsonville, CA, USA). Western blotting equipment and reagents were purchased from Bio-Rad
114 Laboratories (Hercules, CA, USA) and BCA Protein Assay Kit from Peirce (Rockford, IL, USA).
115 Amplex™ Red MAO Assay Kit was purchased from Molecular Probes by Life technologies™
116 (Eugene, OR, USA), and tyramine HCl from Santa Cruz Biotechnology (Dallas, TX, U.S.A.). MAO-
117 Glo™ Kit was purchased from Promega Inc. (Madison, WI, USA).

118 **2.2. Ethanolic Extraction**

119 Plants natural products were extracted for screening for their *h*MAO-A and *h*MAO-B inhibiting
120 potentials, and the top active extracts (potent and selective at 1mg/ml) were further extensively
121 extracted. Briefly, 155 different plant dry parts were used (leaf, stem, root, petal, bark, resin, herb ...,
122 etc.). Each defined amount of 250 mg was grounded to fine powders, homogenized in 99.95%
123 ethanol and macerated once for 50 mg/ml extracts. The top four active plants, of 8 g each, were
124 subject to repeated maceration with mild agitation as the used ethanol solvent was exchanged every

125 24 h and evaporated in a fume hood for ten days to get the crude extract. Only *Ferula assafoetida*
126 resin (FAR) was subject to 80 °C evaporation for a short time using a rotary evaporator to speed
127 drying. All labeled ethanolic extracts (EEs) were stored in air tight glass containers at -20°C in the
128 dark until use.

129 **2.3. Proteins Verification and Method Validation**

130 **2.3.1. Western Blotting**

131 Western blotting was used to verify MAO isozymes. Human dopaminergic neuroblastoma cell line of
132 SH-SY5Y was used as a positive control containing both isozymes, MAO-A [16], and MAO-B, as in
133 the anti-MAO-B datasheet. The cells were obtained from American Type Culture Collection (CRL-
134 2266) (Manassas, VA, USA) and were cultured in DMEM with 10% fetal bovine serum, 100 IU/mL
135 penicillin/streptomycin. To lysate the cells, we used RIPA buffer/protease inhibitor (4°C) with freezing
136 and thawing cycles.

137 To assure equally loaded amounts in micrograms, we performed the BCA protein assay, and the Bio-
138 Tek Synergy HTX Multi-Reader set to 562 nm for analysis. All samples were prepared with 2 x
139 Laemmli sample buffer-2.5% mercaptoethanol loading buffer for 12 µg per lane. Proteins were
140 denatured using heating block for 3-5 min at 100 °C before loading and separated using 1D SDS-
141 PAGE gel electrophoresis of 10%Tris-HCl gradient at 200 V for 55 min. Gels were wetly transferred to
142 nitrocellulose membranes at 100 V for 75 min. Primary antibodies used were rabbit monoclonal anti-
143 MAO-B antibody [EPR7103] (Abcam; ab125010), rabbit monoclonal anti-MAO-A antibody [EPR7101]
144 (Abcam; ab126751) with 1-2:1000 ratio each in cold skim milk. Rabbit anti-β-actin antibody (Abcam;
145 8227) was used for control. Secondary antibodies were goat anti-rabbit IgG H&L HRP-conjugated
146 probes (Abcam; ab6721). The signal was detected using Supersignal[®] West Pico Chemiluminescent
147 Substrate from Thermo Scientific, Pierce Biotechnology (Rockford, IL, USA) and VersaDoc imaging
148 system using CCD camera (Bio-Rad; Hercules, CA, USA)

149 **2.3.2. Substrate Metabolism with Time**

150 In this experiment, substrate concentrations and time required for maximum detectable *h*MAO-A and
151 MAO-B activities were validated; optimal parameters were determined using the continuous Amplex
152 Red fluorometric assay. In brief, *h*MAO-A and B (0.7 U/ml; 0.07 U per reaction) activities were

153 assayed using p-tyramine HCl (tyr.HCl) and benzylamine HCl (benz. HCl) as substrates, respectively.
154 Different substrate volumes of 25 μ L of 4 x the final concentrations were added into black opaque 96-
155 well microplates for their related isozyme assay. Added substrate final concentrations ranged from 0
156 to 0.8 mM with *h*MAO-A, and from 0 to 3 mM with *h*MAO-B, as buffers substituted substrates in
157 control wells. In the dark, the fluorometric reagent was prepared as 4 x the final concentration of 200
158 μ M Amplex Red 1 U/ml and horseradish peroxidase (HRP type-II) in PBS (pH 7.4). Freshly prepared
159 reagent of 25 μ L was added to each well and the reaction was initiated by adding 50 μ L of 2 x
160 isozyme final concentration to the different related substrate concentrations and controls in the wells.
161 Immediately, the fluorescent signal (AFU) of the reactions kinetics with time was read at various time
162 intervals (minutes then hours) at RT. Pre-plate for time zero and post-plate readings for different time
163 intervals were obtained by subtracting the time zero pre-plate reading to monitor the increase as an
164 indicator for the product resorufin continuous accumulation. The AFU excitation resorufin was at 530
165 nm, and its read fluorescence detection was at 590 nm using Synergy HTX Multi-Reader (Bio-Tek).

166 **2.3.3. H₂O₂ Scavenging Activity, Autoxidation, and Resorufin Quenching**

167 Determining maximum H₂O₂ produced within 1 h of incubation at RT was accomplished by
168 interpolating maximum AFU from the H₂O₂ linear standard curve of ranged 0-5 μ M (R² of 99.3%)
169 using GraphPad Prism software. Values of the blank wells without H₂O₂ or enzymes were subtracted
170 from all their corresponding test values. MAO total H₂O₂ production was at a maximum of 0.9 \pm 0.01
171 nmol (4.5 \pm 0.07 μ M). Thus, the scavenging activities were tested for a maximum of 5 μ M at RT.
172 Freshly prepared H₂O₂ was added as 4 x the final concentration to 2 x the final extract concentrations
173 equivalent to MAOs assays. The quenching ability of the Amplex Red product resorufin by the
174 extracts was tested. Based on preliminary studies, resorufin was added as 4 x the final concentration
175 of 20 μ M to 1.3 x the final extract concentrations equivalent to MAOs assays. In autoxidation, the
176 reactions were measured with the same method as scavenging activities except substituting H₂O₂
177 with used reaction buffer and calculated separately as folds of signal increase. Extract tests with
178 high differences from controls are to be eliminated from the MAOs screen assay.

179

180

181 **2.4. *h*MAO-A and *h*MAO-B Fluorometric Microtiter Screening**

182 MAOs activities were assayed using an extremely sensitive continuous fluorometric assay containing
183 Amplex Red (10-acetyl-3, 7-dihydroxyphenoxazine) reagent. The enzymatic H₂O₂ was measured with
184 and without extracts or standards. In addition to random plant selection, some plants were chosen
185 based on our previous work on *h*MAO-B natural inhibitors [17]. Briefly, each of the 155 EEs was
186 diluted in PBS (pH 7.4) in black 96-well microplates to equally make 4 x the final concentration of
187 1mg/ml (n= 2). *h*MAO isozymes on ice with 4 x the final concentration, 0.7 U/ml each, were used. The
188 *h*MAO-A and *h*MAO-B (25 μ L) were separately added to 25 μ L EEs or buffer for control and incubated
189 30-40 min at RT. For the top four extracts IC₅₀s determination, 8 x working solutions in PBS (pH 7.4)
190 were serially diluted for at least ten points before adding the enzymes as mentioned earlier. Control
191 groups were tested with and without maximum ethanol of 1.25%. Buffer solution substituted the
192 enzymes in the correspondent blank wells.

193 The 4 x working solution of Amplex Red reagent was freshly prepared as earlier mentioned in the
194 substrate metabolism optimization method. The previously optimized 4 x the final concentration of 0.5
195 mM tyr. HCl (for *h*MAO-A) and 3 mM benz. HCl (for *h*MAO-B) were prepared. Each substrate was
196 mixed with Amplex Red reagent at 1:1 ratio. A 50 μ L of each mixed solution was added to its
197 corresponding enzyme/extract wells to make the required final extract concentrations. Fluorescent
198 resorufin product was quantified at different time intervals as plates were read at an
199 excitation/emission of 530/590 nm using Synergy HTX Multi-Reader (Bio-Tek, USA). Time zero pre-
200 plate and post-plate readings, at times of 60 min each, were obtained. Percent enzyme inhibition and
201 Relative inhibition (RI_B) were determined for all extracts. In comparison to the related control, any
202 extract that inhibited *h*MAO-B to less than 85% or showed > 1.5-fold ratio RI_B were pointed out. The
203 same was done to the top relative inhibitors against *h*MAO-A (RI_A). Only extracts that ranked the most
204 potent against *h*MAO-B were further evaluated for IC₅₀s as with DEP and pirlindole standard controls.

205 **2.5. Confirmation by a luminescence assay**

206 A luminescence assay, using the MAO-Glo™ Kit, was used with DEP standard to ensure preserved
207 RI_B. Briefly, 12.5 μ L of 4 x the final concentrations of 20 μ g/ml of each extensively extracted plant
208 (PCSEE, PABEE, FAREE, and GUREE) or 5 μ g/ml DEP were added to white opaque 96-well
209 microplates. Fresh 25 μ L of 2 x the final concentration of 0.9 U/ml *h*MAO-A and *h*MAO-B isozymes in

210 reaction buffer (pH 7.4) were incubated with the extracts for 30 min at RT. Controls used were with
211 and without ethanol (0.1%). Reaction buffer substituted each corresponding isozyme to make the
212 blank wells. Based on Valley's method [18] and our preliminary optimizations, 12.5 μ L of 4 x the final
213 concentration of 40 and 4 μ M of luciferin derivative substrate for *hMAO-A* and *hMAO-B* reactions,
214 were added respectively. The reaction was incubated for 60 min at RT. Reporter luciferase detects
215 reagent of 50 μ L per well was added. After 30 min of incubation, produced arbitrary light units (ALU)
216 were detected using Synergy HTX Multi-Reader (Bio-Tek).

217 **2.6. Statistical Analysis**

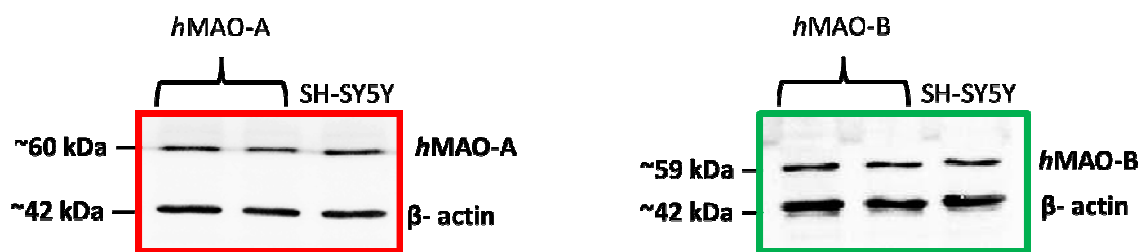
218 Analysis performed by GraphPad Prism Software v6.02 (San Diego, CA, USA). Data points were
219 presented as the mean \pm SEM. IC_{50} s values were interpolated from normalized data by the
220 asymmetric sigmoidal curve and averaged from at least two experiments. One-way and two-way
221 ANOVA were performed followed by multiple comparisons tests to determine the significance of the
222 difference between each two or more groups. In this investigation, relative inhibition (RI_B) which is the
223 ratio of % *hMAO-A* activity/%*hMAO-B* activity at a particular concentration and relative selectivity
224 (RS_B) which is the ratio of *hMAO-A* IC_{50} /*hMAO-B* IC_{50} were measured.

225 **3. RESULTS**

226 **3.1. *hMAO-A* and *hMAO-B* Verification**

227 Both *hMAO-A* and *hMAO-B* identities were verified using Western blotting. The human MAOs
228 antibodies and β -actin Western blotting successfully identified both *hMAO-A* and *hMAO-B* sample
229 proteins at about ~60, ~59, and ~42 KDa, respectively (**Fig. 1**). High intensity detected bands for
230 *hMAO-A* and *hMAO-B* matched the human neuroblastoma SH-SY5Y cells positive controls at their
231 molecular weights.

232

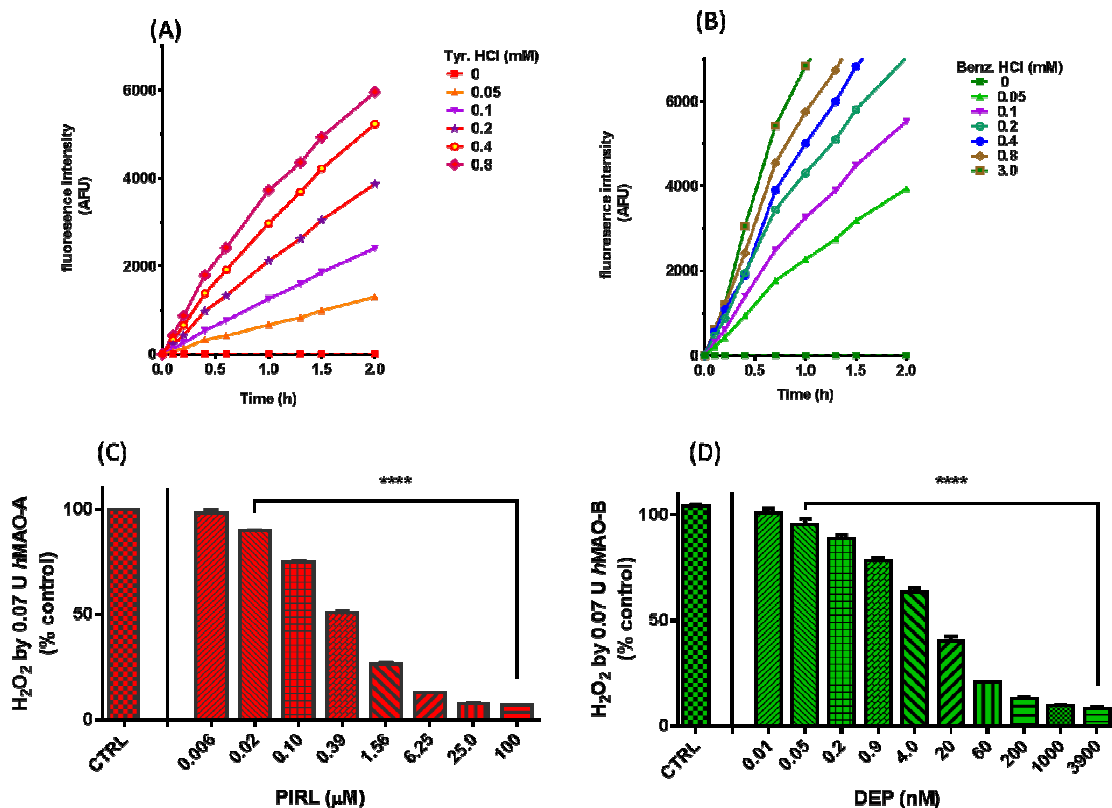


233

234 **Fig. 1.** Verification of the used enzymes *hMAO-A* and *hMAO-B* identities by Western blotting
 235 using equally loaded proteins, and rabbit monoclonal anti-MAO-A, anti-MAO-B and anti-β-
 236 actin antibodies; SH-SY5Y cells (12 μg) were used as positive control for both isozymes.
 237 Bands were detected by HRP-conjugated anti-rabbit secondary antibody.

238 3.2. *hMAO-A* and *hMAO-B* Assay Method Validation

239 To optimize the required time of incubation and substrates concentrations for the used isozymes
 240 amounts, an enzyme-progression curve with different substrate concentrations was performed before
 241 the screening. A proportional increase of AFUs was detected by the used 0.07 U isozyme (0.7 U/ml)
 242 at its initial linear rate of reaction (**Fig. 2**) at RT. AFU, as an H₂O₂ indicator, increased linearly (R²=
 243 99.33%) with a maximum of 6304 ± 25 AFU with time and substrates concentrations within 2 h by
 244 *hMAO-A* (**Fig. 2 A**), and 1 h by *hMAO-B* (**Fig. 2 B**). For optimum isozymes activities, tyr. HCl
 245 concentrations of 0.5 to 0.8 mM (**Fig. 2 A**), and benz. HCl up to 3 mM were required (**Fig. 2 B**). Using
 246 the optimized conditions with standard selective inhibitors of MAO-AI pirlindole and MAO-BI DEP (**Fig.**
 247 **2 C** and **D**); DEP and pirlindole selectively and dose-dependently inhibited their isozymes (DEP
 248 *hMAO-A* IC₅₀= 1.2 ± 0.5 μM and *hMAO-B* IC₅₀= 10 ± 10 nM, and pirlindole *hMAO-A* IC₅₀= 0.24 ± 0.05
 249 μM and *hMAO-B* IC₅₀= 262.2 ± 5.8 μM). To exclude other possible interactions that may interfere with
 250 the *hMAOs* assays, H₂O₂ scavenging, autoxidation, and quenching activities were pre-tested. Any
 251 extract with ≥ 50% scavenging or ≥ 30% quenching activities were excluded from the *hMAO-A* and
 252 *hMAO-B* inhibition extract screenings. Thus, 30 extracts exclusion from the screen.



253

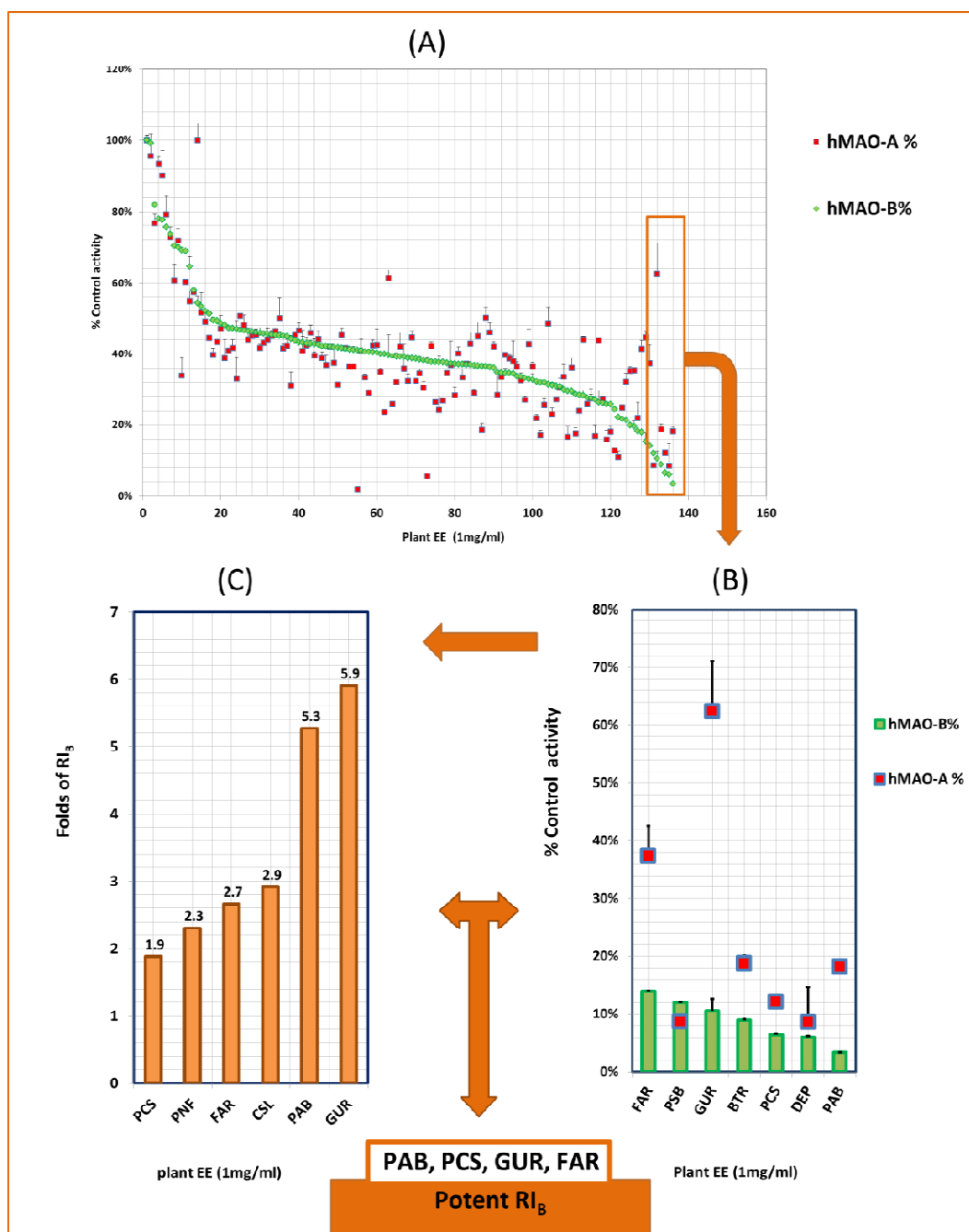
254 **Fig. 2.** Fluorometric assay validation for screening; time and substrate concentration
 255 optimization with **(A)** *hMAO-A* and **(B)** *hMAO-B* isozymes at RT. AFU: Arbitrary
 256 Fluorescence Units. Progression curves with best maximum linearity in the presence of
 257 different substrate concentrations. Optimized conditions of isozymes were inhibited dose-
 258 dependently by selective standard inhibitors: **(C)** MAO-AI pirlindole (PIRL) and **(D)** MAO-BI
 259 deprenyl (DEP). Statistical analysis was presented as the mean ± SEM, n= 3. The
 260 significance of difference between a standard and its control reaction was determined using
 261 one-way ANOVA followed by Dunnett’s multiple comparisons test. **** p < 0.0001.

262 **3.3. Microtiter screening for hMAO-B Relative Inhibition (RI)**

263 To determine the potential of the different plant extracts to exhibit potent RI_B, two separate *hMAO-A*,
 264 and *hMAO-B* inhibition microtiter screenings were conducted using the continuous fluorometric assay
 265 (**Fig. 3**) as previously recommended for HTS [19]. After excluding extracts with the H₂O₂ scavenging
 266 or quenching activities, 132 out of 155 EEs total were tested for both isozymes and ranked as *hMAO-*
 267 *B*Is from low to high (**Fig. 3 A**). The figure shows the different inhibition efficacies and relative
 268 inhibitions; extracts were effective against *hMAO-B* (green dots curved down), *hMAO-A* (red dots
 269 scattered away lower than the green curve), both, or no inhibitions. Interestingly, the screening
 270 elucidated 9% of the 132 plants extract with >1.5-fold *hMAO-B* relative inhibition (RI_B) (**Table 1**), and

271 other 9% of the extracts exerted >1.5-fold *h*MAO-A relative inhibition (RI_A) (**Table 2**). The screen
272 results indicated plants potentials to have significantly collective selective *h*MAO-A and *h*MAO-B
273 inhibiting activities (at least $p = 0.05$). These particular plants may contain more selective *h*MAO-B or
274 *h*MAO-A inhibitors than the ones without different significant inhibitions.

275 The first step in our *h*MAO-B inhibition selectivity screen was to determine potency against the *h*MAO-
276 B activity. The most potent inhibitors of >85% *h*MAO-B activity in **Figure 3 B** ranks were
277 *Phellodendron amurense* barks (PAB) > *Psoralea corylifolia* seeds (PCS) > *Baptisia tinctoria* roots
278 (BTR) > *Glycyrrhiza uralensis* roots (GUR) > *Paeonia suffruticose* roots and barks (PSB) > *Ferula*
279 *assafoetida* resins (FAR). Further in the determination of RI_B , the ranked top RI_B six extracts were
280 partially different (**Fig 3 C**). Although PAB showed the most potent *h*MAO-B inhibition, the extract with
281 the highest RI_B was GUR (5.9-fold). That was followed by PAB, *Camellia sinensis* leaves (CSL), FAR,
282 *Piper nigrum* fruits (PNF), and PCS. From **Figure 3 A & B**, the screened extracts with shared
283 characters of potency against *h*MAO-B and RI_B (PAB, PCS, GUR, and FAR) were selected for further
284 selectivity determination. That method of selection based on the top six ranked screen plants potency
285 and RI_B is to include selective *h*MAO-BIs properties that are hidden by extract potency.



286

287 **Fig. 3.** High Throughput Screening of plants for potent relative inhibitors of recombinant
 288 human monoamine oxidase-B (*hMAO-B*) (RI_B): **(A)** 132 out of 155 extracted plants with
 289 ethanol (1 mg/ml) after hydrogen peroxide scavengers and quenchers excluded. **(B)** The top
 290 potent six extracts inhibited > 85% of *hMAO-B* activity. **(C)** The top six extracts with RI_B
 291 (>1.8-fold). The most potent RI_B extracts in this screen were. *Glycyrrhiza uralensis* (GUR),
 292 *Psoralea corylifolia* seeds (PCS) *Phellodendron amurense* barks (PAB), and *Ferula*
 293 *assafoetida* resin (FAR). Data points compared to standard deprenyl (DEP) are expressed
 294 as mean \pm SEM, with $n=2$. $RI_B = hMAO-A/hMAO-B$.

295

296 **Table 1.** The top relative inhibitors against *h*MAO-B (RI_B) with > 1.5-fold at 1mg/ml plant
 297 ethanolic extract are 12 out of 132 extracted plants. $RI_B = \%hMAO-A/\%hMAO-B$. Significance
 298 of difference between *h*MAO-A and *h*MAO-B% was determined using two-way ANOVA
 299 followed by Sidak's multiple comparisons test. * $p \leq 0.05$, ** $p < 0.01$, *** $p < 0.001$, **** $p <$
 300 0.0001.

Botanical name - part used	<i>h</i>MAO-A ± SEM (%)	<i>h</i>MAO-B ± SEM (%)	Ranked RI_B (fold)	P Level
<i>Glycyrrhiza uralensis</i> - root	62.4 ± 8.6	10.6 ± 2.0	5.9	****
<i>Phellodendron amurense</i> - bark	18.2 ± 1.2	3.5 ± 0.01	5.3	**
<i>Camellia sinensis</i>- leaf	44.6 ± 1.8	15.3 ± 2.5	2.9	****
<i>Ferula assafoetida</i> - resin	37.3 ± 5.2	14.0 ± 0.1	2.7	****
<i>Piper nigrum</i> - fruit	41.4 ± 2.3	18.0 ± 0.3	2.3	****
<i>Baptisia tinctoria</i> - root	18.7 ± 1.3	8.9 ± 0.2	2.1	*
<i>Psoralea corylifolia</i> - seed	12.1 ± 0.7	6.5 ± 0.2	1.9	*
Phoenix dactyliferav- fruit	100.0 ± 4.9	54.3 ± 2.0	1.8	****
<i>Origanum majorana</i> - herb	35.4 ± 0.2	19.6 ± 1.7	1.8	**
<i>Magnolia denudate</i> - flower	35.3 ± 1.1	19.9 ± 0.1	1.8	**
<i>Lycopus lucidus</i> - rhizome	43.8 ± 0.7	26.3 ± 3.3	1.7	***
<i>Curcuma longa</i> - rhizome	44.0 ± 0.8	28.3 ± 1.4	1.6	**

301

302

303

304

305

306

307

308

309

310

311

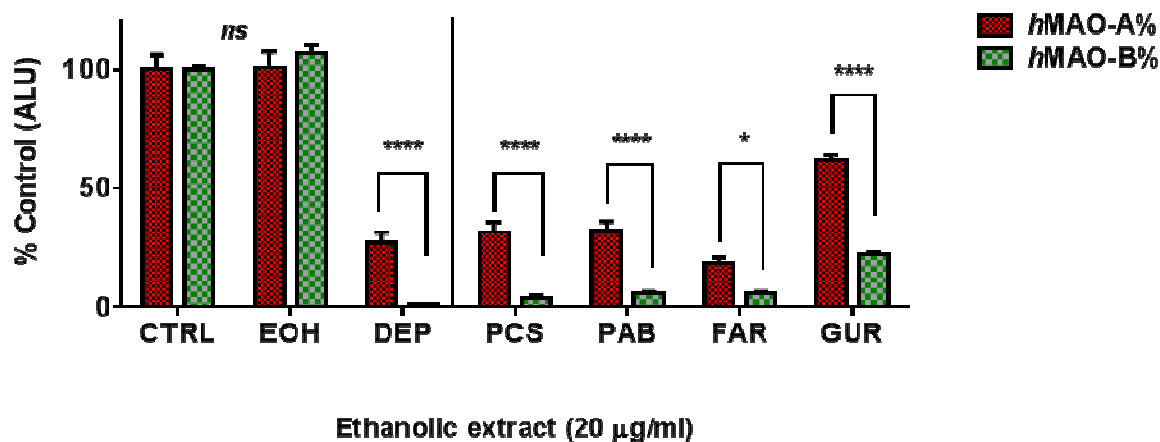
312 **Table 2.** The top relative inhibitors against *h*MAO-A (RI_A) with > 1.5-fold at 1mg/ml plant
 313 ethanolic extract are 11 out of 132 extracted plants. $RI_A = \%hMAO-B/\%hMAO-A$. Significance
 314 of difference between *h*MAO-A and *h*MAO-B% was determined using two-way ANOVA
 315 followed by Sidak's multiple comparisons test. ** $p < 0.01$, *** $p < 0.001$, **** $p < 0.0001$.

<i>Botanical name - part used</i>	<i>h</i> MAO-A ± SEM (%)	<i>h</i> MAO-B ± SEM (%)	Ranked RI_A (fold)	P Level
<i>Clematis trifoliata</i> - fruits	1.8 ± 0.1	41.1 ± 0.3	23.0	****
<i>Dryopteris crassirhizoma</i> - rhizome	5.5 ± 0.1	38.1 ± 0.8	6.9	****
<i>Tilia europaea</i> - leaf	18.5 ± 1.8	36.6 ± 0.5	2.0	****
<i>Zanthoxylum bungeanum</i> - seed	12.8 ± 0.5	24.5 ± 0.2	1.9	***
<i>Lindera aggregata</i> - root	17.1 ± 1.5	32.0 ± 0.2	1.9	****
<i>Laurus nobilis</i> - leaf	16.7 ± 3.0	29.6 ± 0.4	1.8	****
<i>Agrimonia pilosa</i> - herb	23.7 ± 0.2	39.9 ± 0.4	1.7	****
<i>Helichrysum foetidum</i> - flower	17.7 ± 1.4	28.7 ± 0.01	1.6	***
<i>Sargentodoxa cuneate</i> - stem	15.9 ± 2.7	25.8 ± 0.1	1.6	**
<i>Caesalpinia sappan</i> - bark	16.8 ± 3.0	27.2 ± 0.5	1.6	**
<i>Salvia apiana</i> - leaf	24.2 ± 4.0	37.7 ± 1.6	1.6	****

316

317 3.4. Confirmation of Relative *h*MAO-B Inhibition (RI)

318 To confirm the screening results and the preservation of RI_B of the selected top four extracts (GUR,
 319 PAB, PCS, and FAR) after extensive maceration, we used a non- H_2O_2 -dependent luminescence
 320 assay (**Fig. 4**). Used ethanol had no the assay. All tested extensively extracted EEs of only 20 μ g/ml
 321 exerted an equally potent *h*MAO-B inhibition ($p > 0.05$) by > 70% of the 0.4 U isozymes activities.
 322 Moreover, the extracts showed very significant high RI_B activities (8.5-, 5.6-, 3.3-, 2.8-fold for PCS,
 323 PAB, FAR, and GUR, respectively ($p \leq 0.05$ and 0.0001). The results indicate that the screen was
 324 successful in finding potent RI_B s. Also, extracts potencies of inhibition are relatively high and their
 325 selectivities to inhibit *h*MAO-B had not been altered nor masked by the extensive extraction. Notably,
 326 extensive extraction showed an alteration in rankings of extracts with PCS higher potency against
 327 *h*MAO-B ($p < 0.01$) than GUR.

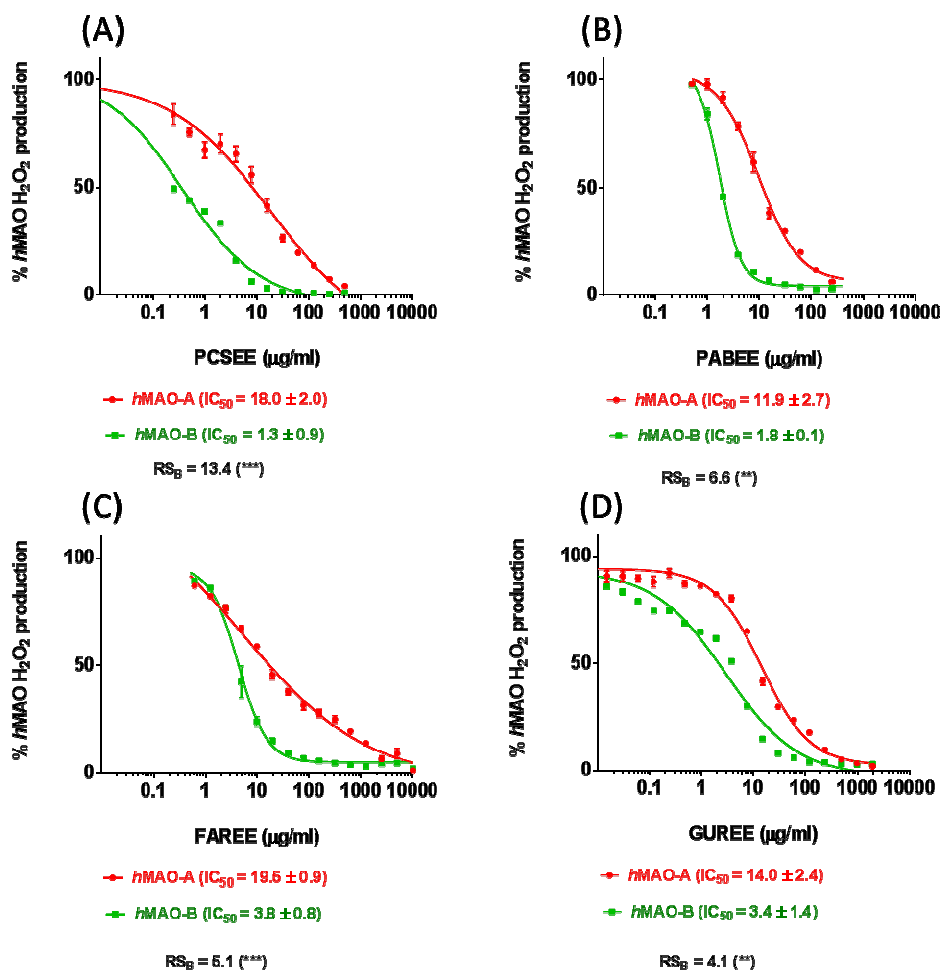


328

329 **Fig. 4.** Luminescence assay confirmation of relative inhibition of *hMAO-B* (RI_B) by
 330 extensively extracted plants of *Psoralea corylifolia* seeds (PCS), *Phellodendron amurense*
 331 (PAB), *Ferula assafoetida* resin (FAR) and *Glycyrrhiza uralensis* (GUR). ALU: arbitrary light
 332 units. Controls activities were compared with ethanol (EOH) and standard MAO-B inhibitor
 333 selegiline (DEP) at 5 $\mu\text{g/ml}$. All four extracts potentially inhibited *hMAO-B* more than *hMAO-A*.
 334 Data points were presented as the mean \pm SEM, with at least $n=3$. The significance of
 335 difference between the two isozymes was determined using two-way ANOVA followed by
 336 Sidak's multiple comparisons test. * $p \leq 0.05$, **** $p < 0.0001$.
 337

338 **3.5. *hMAO-B* Relative Selectivity (RS_B)**

339 To determine the most selective extract among the four extensively macerated plants with ethanol,
 340 the Relative selectivity (RS_B) of each of GUREE, PCSEE, PABEE, and FAREE was investigated
 341 using Amplex Red assay of both isozymes (**Fig. 5**). No significant difference was observed between
 342 controls with and without the used ethanol concentrations. With a similar X-axes scale, all tested EEs
 343 showed a concentration-dependent *hMAO-A* and *hMAO-B* inhibitory potencies with clear RS_B s. The
 344 extracts showed no significant different *hMAO-B* inhibitory potencies from each other ($P > 0.05$).
 345 Nonetheless, the RS_B of each of the four extracts was highly significantly different ($p < 0.01$ and
 346 0.001). Specifically, the most selective *hMAO-B* inhibitors among the four tested EE were PCSEE and
 347 FAREE, with more significant difference RS_B s ($p < 0.001$) than GUREE and PABEE ($p < 0.01$). The
 348 results obtained also indicate preserved RS_B s with increased potencies against *hMAO-B* with the
 349 extensive maceration.



350

351 **Fig. 5.** *hMAO-A* and *hMAO-B* inhibitory potencies and *hMAO-B* relative selectivities (RS_B) of
 352 the extensively macerated ethanolic extracts of **(A)** *Psoralea corylifolia* (PCSEE), **(B)**
 353 *Phellodendron amurense* barks (PABEE), **(C)** *Ferula assafoetida* (FAREE), and **(D)**
 354 *Glycyrrhiza uralensis* (GUREE). All extracts were likewise potent MAOs inhibitors with a
 355 significantly high RS_B . The percent points were presented as the mean \pm SEM, $n = 4$. $IC_{50} \pm$
 356 SEM values were averaged from two experiments. Significance of difference between the
 357 two isozymes IC_{50} s for each extract was determined using two-way ANOVA followed by
 358 Sidak's multiple comparisons test. ** $p < 0.01$, *** $p < 0.001$.

359 **4. DISCUSSION**

360 Plant extracts ability to inhibit human MAO-B selectively was investigated by microtiter screening of
 361 132 ethanolic plant extracts out of the 155 extracts. The initial screen indicates the high potential of
 362 plant extracts that contain varieties of selective *hMAO-B*s, *hMAO-A*s, and non-selective *hMAO*s.
 363 The screen designated the abundance of common selective MAO-A and MAO-B inhibitors in nature.
 364 While it is less relevant for PD and thus beyond the scope of this work investigate *hMAO-A* inhibitors,
 365 our focus was on the plants that specifically inhibit *hMAO-B*. *Psoralea corylifolia* seeds, *Phellodendron*

366 *amurensis* barks, *Glycyrrhiza uralensis* roots, and *Ferula assafoetida* resin ethanolic extracts stood out
367 as potent and selective *h*MAO-B inhibitors. Regardless of their extensive extraction and the used
368 assay, the four extracts consistently showed higher relative *h*MAO-B inhibitions more than *h*MAO-A,
369 which indicates an intrinsic selectivity to inhibit *h*MAO-B. On the other hand, the further extensive
370 extraction dramatically enhanced the potency, particularly at high concentrations. Similar to the used
371 standards of DEP and pirlindole, the high extracts potencies concealed, but did not alter, their
372 preserved *h*MAO-B relative inhibition.

373 The obtained four plant ethanolic extracts preliminary $RI_{B/S}$ and conclusive $RS_{B/S}$ were not due to their
374 effects on H_2O_2 as confirmed with the luminescence assay. H_2O_2 scavenging activities or redox
375 properties would equivalently reduce the total H_2O_2 in both assayed isozymes at the same extract
376 concentration. Also, the H_2O_2 scavenging activity can alter the inhibition selectivity from *h*MAO-B to
377 *h*MAO-A which produces less H_2O_2 at 1 h reaction. The Amplex Red assay used for this screen is a
378 highly sensitive one-step reaction method with a stable detection reagent product. It was previously
379 evaluated for HTS and proposed over other conventional HPLC method for its convenience and
380 continuity [19]. The use of the endogenous substrate tyramine and measuring the cytotoxic enzymes
381 product H_2O_2 is advantageous as it mimics the biological reactions within the body. In contrast with
382 the luminescence assay, *h*MAO-B very high luciferin derivative substrate affinity (4 μ M) may not
383 represent natural neurotransmitters affinities as benz. HCl does in the fluorometric assay. However,
384 our used fluorescence assay led to eliminating many extracts from the screening as it was not suitable
385 to detect MAOIs in extracts with H_2O_2 scavenging activities because of the extract direct interferences
386 with the enzymatic H_2O_2 .

387 In this work, the investigated *Ferula assafoetida* resin (*aka* stinking assa; family Apiaceae) showed
388 high potency and selective inhibition of *h*MAO-B. This resin is used as a spice and a phytomedicine
389 around the globe for centuries. In the folklore medicine, it is mostly used in asthma, gastrointestinal
390 disorders, and neuronal disorders [20]. In recent reports, the resin improved memory and learning in
391 rats [21], and exhibited neuroprotection and nerve stimulation in mice peripheral neuropathy [22], and
392 anticonvulsant properties [23]. FAR contains bioactive phytochemicals such as polysulfides,
393 sesquiterpenes, sesquiterpene-coumarins, diterpenes, phenolics, and flavonoids [20, 24]. Its
394 coumarin umbelliprenin showed anti-inflammatory properties [20], while ferulic acid showed anti-

395 atherosclerotic, antioxidant, and neuroprotective properties [25] and became a candidate for AD [26].
396 Therefore, investigations on the resin concerning PD need to be considered.
397 In addition, the seeds of *Psoralea corylifolia* (aka, Bu Gu Zhi or Babchi; family Leguminosae) are
398 important in traditional Chinese and Ayurvedic medicines [27]. PCSEE was one of the most potent
399 and selective *h*MAO-BI using our fluorometric screening assay. Our PCS findings are supported by
400 our previous investigations on its *h*MAO-B inhibitory potency tested spectrophotometrically [17], and
401 its selectivity for *h*MAO-B using a luminescence assay [28]. Previous PCS screened extracts for
402 active constituents revealed that the ethanolic extract composes more medically active compounds
403 than some other PCS extracts, which makes it a better candidate for novel phytomedicines [29].
404 PSCEE is rich in benzopyrone structure constituents including coumarins and flavonoids. PCS
405 furocoumarins psoralen and isopsoralen showed *rat* MAOs activities inhibitions [30], which was
406 supported by total furocoumarins potent antidepressant effects on mice [31]. PCS also contains
407 isoflavones which have been used as dietary supplements in various diseases, including
408 osteoporosis, cognitive dysfunction, cardiovascular disease, and inflammation [32], which are close to
409 PCS multifaceted properties [33-35]. We previously investigated bavachinin and genistein flavonoids
410 constituents of PCS. Bavachinin exhibited a selective *h*MAO-B inhibition [28] while isoflavone
411 genistein was similarly potent but less selective against *h*MAO-B [36]. Moreover, PCSEE contains
412 monoterpenes that protected against the MAO-B substrate 1-methyl-4-phenyl-1,2,3,6-
413 tetrahydropyridine (MPTP) SN cell damage and MPTP-induced motor deficits in PD model [37],
414 inhibited DA and norepinephrine (NE) transporters [38], and showed antidepressant effects with
415 catecholamine neurotransmitters regulation [39, 40]. The PCS extracts were also neuroprotective
416 against the MPTP precursor MPP+ [38] and the nitropropionic acid (3-NP) induced cytotoxicity and
417 mitochondrial dysfunction [41]. Although the seeds are used in dermatological disorders health
418 supplements [33] and increasingly investigated on *in vitro* and animal models, the extract and its
419 phytochemicals clinical effects on degenerative diseases are yet to be clinically considered. From our
420 results, the observed association between PCS constituents MAO-B inhibitions and the extracts
421 neuroprotection in the previous reports suggests more investigations for potential beneficial PCS
422 phytochemicals for PD.

423 Also, *Phellodendron amurense* (aka Amur cork tree; family Rutaceae) is a meagerly investigated
424 Chinese medicinal plant. In our study, its bark ethanolic extract clearly was a selective *h*MAO-BI as its

425 potent inhibition was previously spectrophotometrically confirmed [17]. The plant constituted alkaloids
426 such as phellodendrine, palmatine, jatrorrhizine, and berberine [42, 43] where the later displayed safe
427 antidepressant-like activities in mice by the possible mechanism MAO-A inhibition and increasing DA,
428 NE and serotonin brain levels [44, 45]. PAB is high in the flavone tetramethyl-o-scutellarin, and the
429 triterpenoids limonoids [42]. Limonoid obacunone was found neuroprotective in glutamate-induced
430 neurotoxicity in vitro [46]. In clinical studies, PAB extract supplement safely reduced cortisol [47], and
431 relieved mild anxiety in women [48]. Also, PAB inhibited pro-inflammatory cytokines [49, 50] and
432 protected from prostate tumors progression [51], property found in some MAO-AIs [52]. Based on our
433 results and literature, there is a lack of knowledge on MAO-B inhibition and selectivity benefits of PAB
434 extracts and phytochemicals. Further studies on PABEE as MAO-BI source for PD are highly
435 recommended.

436 The roots of *Glycyrrhiza uralensis* (aka Chinese licorice; family Leguminosae) is another commonly
437 used medicinal plant in traditional Chinese and natural medicine. Our new finding that GUREE inhibits
438 hMAO-B selectively is supported by our previous finding for its hMAO-B inhibition [17]. Interestingly,
439 GUR was more selective than *Glycyrrhiza glabra* in our screen. Reported *Glycyrrhiza uralensis*
440 different active constituents from other *Glycyrrhiza* genuses may influence its MAO-B selective
441 inhibition [53]. GUR contains unique phytochemicals including isoprenylated phenolics [54] flavonoids,
442 chalcones, and triterpene saponins [55]. Chalcone isoliquiritigenin, is an inhibitor for MAO-B [56] with
443 multifunctional anti-inflammatory, antioxidant, cytoprotective [57] cellular detoxification system
444 activator [58] and anti-apoptotic [59] anti-amyloid- β toxicity [60] neuroprotective properties. GUR total
445 flavonoids extracts showed neurogenesis protective effect in depressed rats model [61]. The flavonoid
446 liquiritin showed antioxidant and antiapoptotic neuroprotective effects in mice [62] and ameliorated
447 depression in rat model [63]. Its benzopyran dehydroglyasperin-C also showed neuroprotection [64].
448 Xiaoyaosan, a traditional herb combination containing GUR for chronic depression, was effective in
449 both animal models and clinical trials [65, 66]. Other multifunctional properties of GUR constituents
450 included reducing pro-inflammatory cytokines, nitric oxide, reactive oxygen species, lipid peroxidation
451 [67], and mitochondrial impairment [68]. Interestingly, GUREE reports covered its chemopreventive
452 [69] and anti-diabetic properties [70]. Specifically investigating GUREE as a selective MAO-BI could
453 be beneficial.

454

455 **5. CONCLUSION**

456 Natural products are abundant of MAOIs with MAO-B selectivity and PCSEE, PABEE, GUREE, and
 457 FAREE are sources of yet to define MAO-B specific natural inhibitors. These plants contain high
 458 varieties of pharmacologically unique active phytochemicals such as coumarins, terpenes, flavonoids,
 459 and alkaloids. Therefore, the current findings may lead to the discovery of novel selective MAO-B
 460 inhibitors to benefit PD patients and beyond. Future research is required to elucidate and understand
 461 the pharmacological actions of these extracts and their phytochemicals which are responsible for the
 462 selectivity of hMAO-B inhibition and, consequently, finding safe therapeutic compounds for
 463 neurodegenerative diseases such as PD.

464 **REFERENCES**

- 465 [1] Mallajosyula, J.K., D. Kaur, S.J. Chinta, S. Rajagopalan, A. Rane, D.G. Nicholls, et
 466 al., MAO-B elevation in mouse brain astrocytes results in Parkinson's pathology.
 467 PLoS One, 2008; 32: p. e1616.
- 468 [2] Youdim, M.B. and J.J. Buccafusco, Multi-functional drugs for various CNS targets in
 469 the treatment of neurodegenerative disorders. Trends Pharmacol Sci, 2005; 261: p.
 470 27-35.
- 471 [3] Reis, J., I. Encarnacao, A. Gaspar, A. Morales, N. Milhazes and F. Borges,
 472 Parkinson's disease management. Part II-Discovery of MAO-B inhibitors based on
 473 nitrogen heterocycles and analogs. Curr Top Med Chem, 2012; 1220: p. 2116-30.
- 474 [4] Saura, J., J.M. Luque, A.M. Cesura, M.D. Prada, V. Chan-Palay, G. Huber, et al.,
 475 Increased monoamine oxidase b activity in plaque-associated astrocytes of
 476 Alzheimer brains revealed by quantitative enzyme radioautography. Neuroscience,
 477 1994; 621: p. 15-30.
- 478 [5] Damier, P., A. Kastner, Y. Agid and E.C. Hirsch, Does monoamine oxidase type B
 479 play a role in dopaminergic nerve cell death in Parkinson's disease? Neurology,
 480 1996; 465: p.1262-1262.
- 481 [6] Wood, P.L., M.A. Khan, S.R. Kulow, S.A. Mahmood and J.R. Moskal, Neurotoxicity of
 482 reactive aldehydes: the concept of "aldehyde load" as demonstrated by
 483 neuroprotection with hydroxylamines. Brain Res, 2006; 10951: p. 190-9.
- 484 [7] Grunblatt, E., S. Mandel, J. Jacob-Hirsch, S. Zeligson, N. Amariglio, G. Rechavi, et
 485 al., Gene expression profiling of parkinsonian substantia nigra pars compacta;
 486 alterations in ubiquitin-proteasome, heat shock protein, iron and oxidative stress-
 487 regulated proteins, cell adhesion/cellular matrix and vesicle trafficking genes. J
 488 Neural Transm (Vienna), 2004; 11112: p. 1543-73.
- 489 [8] Youdim, M.B. and Y.S. Bakhle, Monoamine oxidase: isoforms and inhibitors in
 490 Parkinson's disease and depressive illness. Br J Pharmacol, 2006; 147 Suppl 1: p.
 491 S287-96.
- 492 [9] Finberg, J.P. and K. Gillman, Selective inhibitors of monoamine oxidase type B and
 493 the "cheese effect". Int Rev Neurobiol, 2011; 100: p. 169-90.
- 494 [10] Shulman, K.I., N. Herrmann and S.E. Walker, Current place of monoamine oxidase
 495 inhibitors in the treatment of depression. CNS Drugs, 2013; 2710: p. 789-97.
- 496 [11] Song, M.S., D. Matveychuk, E.M. MacKenzie, M. Duchcherer, D.D. Mousseau and
 497 G.B. Baker, An update on amine oxidase inhibitors: multifaceted drugs. Prog
 498 Neuropsychopharmacol Biol Psychiatry, 2013; 44: p. 118-24.

- 499 [12] Ebadi, M., H. Brown-Borg, J. Ren, S. Sharma, S. Shavali, H. El ReFaey, et al.,
500 Therapeutic efficacy of selegiline in neurodegenerative disorders and neurological
501 diseases. *Curr Drug Targets*, 2006; 711: p. 1513-29.
- 502 [13] Bar Am, O., T. Amit and M.B. Youdim, Contrasting neuroprotective and neurotoxic
503 actions of respective metabolites of anti-Parkinson drugs rasagiline and selegiline.
504 *Neurosci Lett*, 2004; 3553: p. 169-72.
- 505 [14] Vartzopoulos, D. and F. Krull, Dependence on monoamine oxidase inhibitors in high
506 dose. *Br J Psychiatry*, 1991; 158: p. 856-7.
- 507 [15] Carradori, S., M. D'Ascenzio, P. Chimenti, D. Secci and A. Bolasco, Selective MAO-
508 B inhibitors: a lesson from natural products. *Mol Divers*, 2014; 181: p. 219-43.
- 509 [16] Cao, X., X.M. Li and D.D. Mousseau, Calcium alters monoamine oxidase-A
510 parameters in human cerebellar and rat glial C6 cell extracts: possible influence by
511 distinct signaling pathways. *Life Sci*, 2009; 855-6: p. 262-8.
- 512 [17] Mazzio, E., S. Deiab, K. Park and K.F. Soliman, High throughput screening to identify
513 natural human monoamine oxidase B inhibitors. *Phytother Res*, 2013; 276: p. 818-
514 28.
- 515 [18] Valley, M.P., W. Zhou, E.M. Hawkins, J. Shultz, J.J. Cali, T. Worzella, et al., A
516 bioluminescent assay for monoamine oxidase activity. *Anal Biochem*, 2006; 3592: p.
517 238-46.
- 518 [19] Guang, H.M. and G.H. Du, High-throughput screening for monoamine oxidase-A and
519 monoamine oxidase-B inhibitors using one-step fluorescence assay. *Acta Pharmacol*
520 *Sin*, 2006; 276: p. 760-6.
- 521 [20] Iranshahy, M. and M. Iranshahi, Traditional uses, phytochemistry and pharmacology
522 of asafoetida (*Ferula assa-foetida* oleo-gum-resin)-a review. *J Ethnopharmacol*,
523 2011; 1341: p. 1-10.
- 524 [21] Vijayalakshmi, S. Adiga, P. Bhat, A. Chaturvedi, K.L. Bairy and S. Kamath,
525 Evaluation of the effect of *Ferula asafoetida* Linn. gum extract on learning and
526 memory in Wistar rats. *Indian J Pharmacol*, 2012; 441: p. 82-7.
- 527 [22] Homayouni Moghadam, F., M. Dehghan, E. Zarepur, R. Dehlavi, F. Ghaseminia, S.
528 Ehsani, et al., Oleo gum resin of *Ferula assa-foetida* L. ameliorates peripheral
529 neuropathy in mice. *J Ethnopharmacol*, 2014; 1541: p. 183-9.
- 530 [23] Bagheri, S.M., M.E. Rezvani, A.R. Vahidi and M. Esmaili, Anticonvulsant effect of
531 *ferula assa-foetida* oleo gum resin on chemical and amygdala-kindled rats. *N Am J*
532 *Med Sci*, 2014; 68: p. 408-12.
- 533 [24] Kavooosi, G. and V. Rowshan, Chemical composition, antioxidant and antimicrobial
534 activities of essential oil obtained from *Ferula assa-foetida* oleo-gum-resin: Effect of
535 collection time. *Food Chemistry*, 2013; 1384: p. 2180-2187.
- 536 [25] Cheng, C.Y., S.Y. Su, N.Y. Tang, T.Y. Ho, S.Y. Chiang and C.L. Hsieh, Ferulic acid
537 provides neuroprotection against oxidative stress-related apoptosis after cerebral
538 ischemia/reperfusion injury by inhibiting ICAM-1 mRNA expression in rats. *Brain Res*,
539 2008; 1209: p. 136-50.
- 540 [26] Sgarbossa, A., D. Giacomazza and M. di Carlo, Ferulic Acid: A Hope for Alzheimer's
541 Disease Therapy from Plants. *Nutrients*, 2015; 77: p. 5764-82.
- 542 [27] Khushboo, P.S., V.M. Jadhav, V.J. Kadam and N.S. Sathe, *Psoralea corylifolia* Linn.-
543 "Kushtanashini". *Pharmacogn Rev*, 2010; 47: p. 69-76.
- 544 [28] Zarmouh, N.O., E.A. Mazzio, F.M. Elshami, S.S. Messeha, S.V.K. Eyunni and K.F.A.
545 Soliman, Evaluation of the Inhibitory Effects of Bavachinin and Bavachin on Human
546 Monoamine Oxidases A and B. *Evid-Based Complement and Alternat Med*, 2015;
547 2015: p. 14.
- 548 [29] RafiqKhan, M. and R. Ranjini, Preliminary phytochemical screening of seeds of
549 *Psoralea corylifolia*. *Int Res J Pharm*, 2013; 41: p. 129-130.
- 550 [30] Kong, L.D., R.X. Tan, A.Y. Woo and C.H. Cheng, Inhibition of rat brain monoamine
551 oxidase activities by psoralen and isopsoralen: implications for the treatment of
552 affective disorders. *Pharmacol Toxicol*, 2001; 882: p. 75-80.

- 553 [31] Chen, Y., L.D. Kong, X. Xia, H.F. Kung and L. Zhang, Behavioral and biochemical
554 studies of total furocoumarins from seeds of *Psoralea corylifolia* in the forced
555 swimming test in mice. *J Ethnopharmacol*, 2005; 963: p. 451-9.
- 556 [32] Lu, T.M., H.H. Ko, L.T. Ng and Y.P. Hsieh, Free-Radical-Scavenging, Antityrosinase,
557 and Cellular Melanogenesis Inhibitory Activities of Synthetic Isoflavones. *Chem*
558 *Biodivers*, 2015; 126: p. 963-79.
- 559 [33] Chopra, B., A.K. Dhingra and K.L. Dhar, *Psoralea corylifolia* L. (Buguchi) - folklore to
560 modern evidence: a review. *Fitoterapia*, 2013; 90: p. 44-56.
- 561 [34] Backhouse, C.N., C.L. Delporte, R.E. Negrete, S. Erazo, A. Zuniga, A. Pinto, et al.,
562 Active constituents isolated from *Psoralea glandulosa* L. with anti-inflammatory and
563 antipyretic activities. *J Ethnopharmacol*, 2001; 781: p. 27-31.
- 564 [35] Lee, M.H., J.Y. Kim and J.H. Ryu, Prenylflavones from *Psoralea corylifolia* inhibit
565 nitric oxide synthase expression through the inhibition of I-kappaB-alpha degradation
566 in activated microglial cells. *Biol Pharm Bull*, 2005; 2812: p. 2253-7.
- 567 [36] Zarmouh, N.O., S.S. Messeha, F.M. Elshami and K.F. Soliman, Evaluation of the
568 Isoflavone Genistein as Reversible Human Monoamine Oxidase-A and-B Inhibitor.
569 *Evidence-Based Complementary and Alternative Medicine*, 2016; 2016.
- 570 [37] Zhao, G., X.W. Zheng, G.W. Qin, Y. Gai, Z.H. Jiang and L.H. Guo, In vitro
571 dopaminergic neuroprotective and in vivo antiparkinsonian-like effects of Delta 3,2-
572 hydroxybakuchiol isolated from *Psoralea corylifolia* (L.). *Cell Mol Life Sci*, 2009; 669:
573 p. 1617-29.
- 574 [38] Zhao, G., S. Li, G.W. Qin, J. Fei and L.H. Guo, Inhibitive effects of *Fructus Psoraleae*
575 extract on dopamine transporter and noradrenaline transporter. *J Ethnopharmacol*,
576 2007; 1123: p. 498-506.
- 577 [39] Yi, L.T., Y.C. Li, Y. Pan, J.M. Li, Q. Xu, S.F. Mo, et al., Antidepressant-like effects of
578 psoralidin isolated from the seeds of *Psoralea Corylifolia* in the forced swimming test
579 in mice. *Prog Neuropsychopharmacol Biol Psychiatry*, 2008; 322: p. 510-9.
- 580 [40] Mao, H., H. Wang, S. Ma, Y. Xu, H. Zhang, Y. Wang, et al., Bidirectional regulation of
581 bakuchiol, an estrogenic-like compound, on catecholamine secretion. *Toxicol Appl*
582 *Pharmacol*, 2014; 2741: p. 180-9.
- 583 [41] Im, A.R., S.W. Chae, G.J. Zhang and M.Y. Lee, Neuroprotective effects of *Psoralea*
584 *corylifolia* Linn seed extracts on mitochondrial dysfunction induced by 3-
585 nitropropionic acid. *BMC Complement Altern Med*, 2014; 14: p. 370.
- 586 [42] Sun, H., H. Wang, A. Zhang, G. Yan, Y. Han, Y. Li, et al., Chemical Discrimination of
587 *Cortex Phellodendri amurensis* and *Cortex Phellodendri chinensis* by Multivariate
588 Analysis Approach. *Pharmacogn Mag*, 2016; 1245: p. 41-9.
- 589 [43] Yang, Q., F. Zhang, S.H. Gao, L.N. Sun and W.S. Chen, Determination of bioactive
590 compounds in *Cortex Phellodendri* by high-performance liquid chromatography. *J*
591 *AOAC Int*, 2010; 933: p. 855-61.
- 592 [44] Peng, W.H., K.L. Lo, Y.H. Lee, T.H. Hung and Y.C. Lin, Berberine produces
593 antidepressant-like effects in the forced swim test and in the tail suspension test in
594 mice. *Life Sci*, 2007; 8111: p. 933-8.
- 595 [45] Kulkarni, S.K. and A. Dhir, On the mechanism of antidepressant-like action of
596 berberine chloride. *Eur J Pharmacol*, 2008; 5891-3: p. 163-72.
- 597 [46] Tanaka, T., H. Kohno, Y. Tsukio, S. Honjo, M. Tanino, M. Miyake, et al., Citrus
598 limonoids obacunone and limonin inhibit azoxymethane-induced colon
599 carcinogenesis in rats. *Biofactors*, 2000; 131-4: p. 213-8.
- 600 [47] Talbott, S.M., J.A. Talbott and M. Pugh, Effect of *Magnolia officinalis* and
601 *Phellodendron amurense* (Relora(R)) on cortisol and psychological mood state in
602 moderately stressed subjects. *J Int Soc Sports Nutr*, 2013; 101: p. 37.
- 603 [48] Kalman, D.S., S. Feldman, R. Feldman, H.I. Schwartz, D.R. Krieger and R. Garrison,
604 Effect of a proprietary *Magnolia* and *Phellodendron* extract on stress levels in healthy
605 women: a pilot, double-blind, placebo-controlled clinical trial. *Nutr J*, 2008; 7: p. 11.

- 606 [49] Kim, J.H., J.E. Huh, Y.H. Baek, J.D. Lee, D.Y. Choi and D.S. Park, Effect of
607 Phellodendron amurense in protecting human osteoarthritic cartilage and
608 chondrocytes. *J Ethnopharmacol*, 2011; 1342: p. 234-42.
- 609 [50] Xian, Y.F., Q.Q. Mao, S.P. Ip, Z.X. Lin and C.T. Che, Comparison on the anti-
610 inflammatory effect of Cortex Phellodendri Chinensis and Cortex Phellodendri
611 Amurensis in 12-O-tetradecanoyl-phorbol-13-acetate-induced ear edema in mice. *J*
612 *Ethnopharmacol*, 2011; 1373: p. 1425-30.
- 613 [51] Ghosh, R., H. Graham, P. Rivas, X.J. Tan, K. Crosby, S. Bhaskaran, et al.,
614 Phellodendron amurense bark extract prevents progression of prostate tumors in
615 transgenic adenocarcinoma of mouse prostate: potential for prostate cancer
616 management. *Anticancer Res*, 2010; 303: p. 857-65.
- 617 [52] Flamand, V., H. Zhao and D.M. Peehl, Targeting monoamine oxidase A in advanced
618 prostate cancer. *J Cancer Res Clin Oncol*, 2010; 13611: p. 1761-71.
- 619 [53] Hatano, T., T. Fukuda, Y.Z. Liu, T. Noro and T. Okuda, [Phenolic constituents of
620 licorice. IV. Correlation of phenolic constituents and licorice specimens from various
621 sources, and inhibitory effects of licorice extracts on xanthine oxidase and
622 monoamine oxidase]. *Yakugaku Zasshi*, 1991; 1116: p. 311-21.
- 623 [54] Ji, S., Z. Li, W. Song, Y. Wang, W. Liang, K. Li, et al., Bioactive Constituents of
624 Glycyrrhiza uralensis (Licorice): Discovery of the Effective Components of a
625 Traditional Herbal Medicine. *J Nat Prod*, 2016; 792: p. 281-92.
- 626 [55] Lee, J.E., J.Y. Lee, J. Kim, K. Lee, S.U. Choi and S.Y. Ryu, Two minor chalcone
627 acetylglycosides from the roots extract of Glycyrrhiza uralensis. *Arch Pharm Res*,
628 2015; 387: p. 1299-303.
- 629 [56] Tanaka, S., Y. Kuwai and M. Tabata, Isolation of monoamine oxidase inhibitors from
630 Glycyrrhiza uralensis roots and the structure-activity relationship. *Planta Med*, 1987;
631 531: p. 5-8.
- 632 [57] Peng, F., Q. Du, C. Peng, N. Wang, H. Tang, X. Xie, et al., A Review: The
633 Pharmacology of Isoliquiritigenin. *Phytother Res*, 2015; 297: p. 969-77.
- 634 [58] Gong, H., B.K. Zhang, M. Yan, P.F. Fang, H.D. Li, C.P. Hu, et al., A protective
635 mechanism of licorice (*Glycyrrhiza uralensis*): isoliquiritigenin stimulates
636 detoxification system via Nrf2 activation. *J Ethnopharmacol*, 2015; 162: p. 134-9.
- 637 [59] Hwang, C.K. and H.S. Chun, Isoliquiritigenin isolated from licorice *Glycyrrhiza*
638 *uralensis* prevent 6-hydroxydopamine-induced apoptosis in dopaminergic neurons.
639 *Biosci Biotechnol Biochem*, 2012; 763: p. 536-43.
- 640 [60] Link, P., B. Wetterauer, Y. Fu and M. Wink, Extracts of *Glycyrrhiza uralensis* and
641 isoliquiritigenin counteract amyloid-beta toxicity in *Caenorhabditis elegans*. *Planta*
642 *Med*, 2015; 815: p. 357-62.
- 643 [61] Fan, Z.Z., W.H. Zhao, J. Guo, R.F. Cheng, J.Y. Zhao, W.D. Yang, et al.,
644 [Antidepressant activities of flavonoids from *Glycyrrhiza uralensis* and its
645 neurogenesis protective effect in rats]. *Yao Xue Xue Bao*, 2012; 4712: p. 1612-7.
- 646 [62] Sun, Y.X., Y. Tang, A.L. Wu, T. Liu, X.L. Dai, Q.S. Zheng, et al., Neuroprotective
647 effect of liquiritin against focal cerebral ischemia/reperfusion in mice via its
648 antioxidant and antiapoptosis properties. *J Asian Nat Prod Res*, 2010; 1212: p. 1051-
649 60.
- 650 [63] Zhao, Z., W. Wang, H. Guo and D. Zhou, Antidepressant-like effect of liquiritin from
651 *Glycyrrhiza uralensis* in chronic variable stress induced depression model rats.
652 *Behav Brain Res*, 2008; 1941: p. 108-13.
- 653 [64] Kim, H.J., S.S. Lim, I.S. Park, J.S. Lim, J.Y. Seo and J.S. Kim, Neuroprotective
654 effects of dehydroglyasperin C through activation of heme oxygenase-1 in mouse
655 hippocampal cells. *J Agric Food Chem*, 2012; 6022: p. 5583-9.
- 656 [65] Dai, Y., Z. Li, L. Xue, C. Dou, Y. Zhou, L. Zhang, et al., Metabolomics study on the
657 anti-depression effect of xiaoyaosan on rat model of chronic unpredictable mild
658 stress. *J Ethnopharmacol*, 2010; 1282: p. 482-9.
- 659 [66] Tian, J.S., G.J. Peng, X.X. Gao, Y.Z. Zhou, J. Xing, X.M. Qin, et al., Dynamic
660 analysis of the endogenous metabolites in depressed patients treated with TCM

- 661 formula Xiaoyaosan using urinary (1)H NMR-based metabolomics. J
662 Ethnopharmacol, 2014; 158 Pt A: p. 1-10.
- 663 [67] Fu, Y., J. Chen, Y.J. Li, Y.F. Zheng and P. Li, Antioxidant and anti-inflammatory
664 activities of six flavonoids separated from licorice. Food Chem, 2013; 1412: p. 1063-
665 71.
- 666 [68] Yang, E.J., J.S. Min, H.Y. Ku, H.S. Choi, M.K. Park, M.K. Kim, et al., Isoliquiritigenin
667 isolated from Glycyrrhiza uralensis protects neuronal cells against glutamate-induced
668 mitochondrial dysfunction. Biochem Biophys Res Commun, 2012; 4214: p. 658-64.
- 669 [69] Jo, E.H., S.H. Kim, J.C. Ra, S.R. Kim, S.D. Cho, J.W. Jung, et al., Chemopreventive
670 properties of the ethanol extract of Chinese licorice (*Glycyrrhiza uralensis*) root:
671 induction of apoptosis and G1 cell cycle arrest in MCF-7 human breast cancer cells.
672 Cancer Lett, 2005; 2302: p. 239-47.
- 673 [70] Mae, T., H. Kishida, T. Nishiyama, M. Tsukagawa, E. Konishi, M. Kuroda, et al., A
674 licorice ethanolic extract with peroxisome proliferator-activated receptor-gamma
675 ligand-binding activity affects diabetes in KK-Ay mice, abdominal obesity in diet-
676 induced obese C57BL mice and hypertension in spontaneously hypertensive rats. J
677 Nutr, 2003; 13311: p. 3369-77.
- 678